Synthesis, Crystal Structure of *Cis*-dioxo-catecholatotungsten (VI) Complex and Its NMR Studies on the Interaction with ATP

LU, Xiao-Ming*,[a](鲁晓明) LIU, Shun-Cheng[a](刘顺成) JIANG, Ling[b](姜凌)
MAO, Xi-An[b](毛希安) YE, Zhao-Hui[b](叶朝晖)
[a] *Department of Chemistry, Capital Normal University, Beijing 100037, China*
[b] *Wuhan Institute of Physics and Mathematics, Chinese Academy of Sciences, Wuhan, Hubei 430071, China*

***Cis*-dioxo-catecholatotungsten (VI) complex anion $[W^{(VI)}O_2(OC_6H_4O)_2]^{2-}$ was obtained with discrete protonated ethylenediamine $(NH_2CH_2CH_2NH_3)^+$ cations by the reaction of tetrabutyl ammonium decatungstate with catechol in the mixed solvent of CH_3OH, CH_3CN and ethylenediamine, and compared with its molybdenum analogue $[Mo^{(V)}O_2(OC_6H_4O)_2]^{3-}$ by crystal structure, UV, EPR. The results of the UV and EPR spectra show that tungsten is less redox active than molybdenum since the molybdenum is reduced from Mo(VI) to Mo(V) but tungsten stays in the original highest oxidized state Mo(VI) when they are crystallized from the solution above. It is worthy to note that $[W^{(VI)}O_2(OC_6H_4O)_2]^{2-}$ shows the same coordination structure as its molybdenum analogue in which the metal center exhibits distorted octahedral coordination geometry with two *cis*-dioxocatecholate ligands and might have the related coordination structure feature with the cofactor of flavoenzyme because $[Mo^{(V)}O_2(OC_6H_4O)_2]^{3-}$ presented essentially the same EPR spectra as flavoenzyme. The NMR studies on the interaction of the title complex with ATP reveal that the reduction of W(VI) to W(V) occurs when the title complex is dissolved in D_2O and the W(V) is oxidized again when ATP solution is mixed with original solution and the hydrolysis of the catecholato ligand take places at mean time being monitored by ^1H NMR and ^{13}C NMR spectra.**

Keywords *cis*-dioxo-catecholatotungsten (VI), EPR, NMR, ATP, DNA cleavage

Introduction

Although tungsten and molybdenum are chemical analogous elements, W and Mo provide a fascinating study area from biological perspective, to our knowledge. However, while molybdenum chemistry is well developed and numerous oxomolybdenum complexes with a range of supporting ligands have been studied extensively the chemistry of analogous tungsten complex remains relatively little studied.[1-5] Until recently, rather dramatic progress has been made in the study of tungstoenzymes, of which the crystal structure of a tungstoenzyme has been determined to 0.23 nm resolution and the direct comparisons of the atomic level between tungstoenzyme and molybdoenzyme are now possible.[6-9]

We have described the synthesis of $(NH_2CH_2CH_2NH_3)_3[Mo^{(V)}O_2(OC_6H_4O)_2]$ in which the metal center exhibits distorted octahedral coordination with two *cis*-dioxocatecholate ligands and the complex shows the similar EPR signal to flavoenzyme which suggests that the complex might have the related coordination structure feature with the Mo-cofactor of flavoenzyme.[10] Herein we described the synthesis of its tungsten analogue $(NH_2CH_2CH_2NH_3)_2[W^{(VI)}O_2(OC_6H_4O)_2]$, made a comparison between them by crystal structure, UV, EPR spectra, and studied the interaction of the title complex with ATP by ^1H NMR and ^{13}C NMR spectra.

Experimental

Material and methods

All reagents used were obtained from commercial supplies. All manipulations were carried out in the laboratory atmosphere. UV-vis spectra were recorded in 10 mm quartz cell on a shimadzu UV-265 instrument. EPR spectrum was measured with Bruck-300 EPR spectrometer. NMR was determined on Bruck-500 NMR spectrometer.

Synthesis of $(NH_2CH_2CH_2NH_3)_2[W^{(VI)}O_2(OC_6H_4O)_2]$

To a 40 mL solution of 25 g $Na_2WO_4\cdot 2H_2O$ prejusted to pH 3.5 with chloric acid, 8 g of $(n\text{-}Bu)_4NBr$ was added and stirred for 1 h, then a white powder of tetra-*n*-butyl ammonium decatungstate was produced, filtered and dried in the air.

A mixture of 0.8 g of catechol and 0.4 g of tetra-*n*-butyl ammonium decatungstate produced above in the mixed solvent of 15 mL of CH_3OH, 15 mL of CH_3CN and

* E-mail: lu-xiaoming@263.net
Received October 15, 2002; revised December 26, 2002; accepted February 24, 2003.
Project supported by the National Natural Science Foundation of China (No. 20271034) and the Natural Science Foundation of Beijing (No. 2012005) and the Natural Science Foundation of Educational Ministry of Beijing.

2 mL of $NH_2CH_2CH_2NH_2$ was stirred for 6 h and filtered, the filtrate was layered with Et_2O for 15 d and yellow crystals were obtained.

The synthesis of $(NH_2CH_2CH_2NH_3)_3[Mo^{(V)}O_2(OC_6H_4O)_2]$ and its crystal structure are presented in paper.[10]

Crystal structure determination

X-Ray data of the tungsten complex were collected on a Enraf-Nonius CAD4 diffractometer using graphite monochromated Mo Kα radiation. An empirical absorption correction using the program DIFABS was applied. The structure was solved by Patterson methods. Non-hydrogen atoms were refined anisotropically and hydrogen atoms were refined isotropically. All calculations were performed on *F* using SHELXTL PLUS (VMS).

NMR *experiment*

The pure samples (ATP and the title complex) were prepared by resolving the crystal in 0.5 mL of D_2O with the concentration of 30 mmol/L respectively, of which complete dissolution can be achieved. The mixtures were prepared by adding 1/2 pure complex solution to 0.5 mL of 30 mmoL/L pure ATP solution, so the ratio of the complex to ATP was 1∶2, that is 10 mmol·L^{-1}∶20 mmol·L^{-1}. Samples were handled without rigorous exclusion of oxygen under 298.2 K, because we wished to mimic the condition used in biological testing. ^1H NMR and ^{13}C NMR spectra of pure and mixed with ATP in solution have been recorded for the title complex respectively.

As the aim of this work was to study the interaction between the complex and ATP at approximately physiological pH, the pD of the solution was maintained in the range of 6.5—7.5. Actually the pD of the solution do not need to be adjusted because the dissolution of ATP and complexes together gives neutral solution naturally (pD is about 7.0).

Results and discussion

Crystal data and experimental details of $(NH_2CH_2CH_2NH_3)_2[W^{(VI)}O_2(OC_6H_4O)_2]$ are listed in Table 1. The selected bond lengths and angles are tabulated in Table 2. The structure of $[W^{(VI)}O_2(OC_6H_4O)_2]^{2-}$ anion is shown in Fig. 1. The packing diagram of the title complex is presented in Fig. 2.

As illustrated in Fig. 1, the structure of the mononuclear anionic units $[W^{(VI)}O_2(OC_6H_4O)_2]^{2-}$ displays the *cis*-dioxo fashion with pseudo-octahedral $[WO_6]$ coordination geometry. The W = O band distances [0.1741(5)—0.1744(5) nm] are within the range of typical oxotungsten units and only marginally longer (by 0.0035—0.0039 nm) than the Mo = O bands [0.1702(6)—0.1709(5) nm] in the molybdenum analogue.[10] Similar to $[Mo^{(V)}O_2(OC_6H_4O)_2]^{3-}$, the *trans* influence of the oxo groups is evident in the nonequivalent W—O (ligand) distances, averaging 0.1982(5) and 0.2131(5) nm for *cis* and *trans* ligation to the oxo groups respectively, and the bond distances are little shorter than Mo—O single distances [0.2012(6)—0.2149(6) nm] respectively. Since $[W^{(VI)}O_2(OC_6H_4O)_2]^{2-}$ is a dinegative anion, two protonated ethylenediamine $(NH_2CH_2CH_2NH_3)^+$ cations are needed to satisfy the charge requirements of the complex anion. It is notable that the substitution of tungsten for molybdenum has little influence on the overall coordination structure though the valences of the central metal are different between $[W^{(VI)}O_2(OC_6H_4O)_2]^{2-}$ and its analogue $[Mo^{(V)}O_2(OC_6H_4O)_2]^{3-}$.

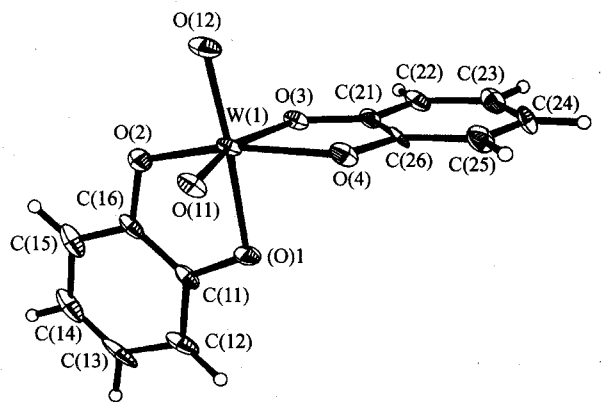

Fig. 1 Structure of $[W^{(VI)}O_2(OC_6H_4O)_2]^{2-}$.

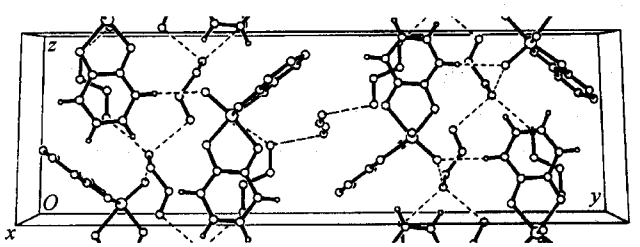

Fig. 2 Packing diagram of $(NH_2CH_2CH_2NH_3)_2[W^{(VI)}O_2(OC_6H_4O)_2]$.

Because there is a unpaired electron in Mo(V) with d^1 electronic configuration while there is no any single electrons in W(VI) with d^1 electronic configuration, it can be supposed that the responses of the two complexes to EPR are quite different. The supposition is confirmed by the EPR experiments, of which $[Mo^{(V)}O_2(OC_6H_4O)_2]^{3-}$ is active response to the EPR while its analogue $[W^{(VI)}O_2(OC_6H_4O)_2]^{2-}$ is EPR silent. It is noteworthy that $[Mo^{(V)}O_2(OC_6H_4O)_2]^{3-}$ gives essentially the same EPR signals as flavoenzyme shown in Fig. 3, which implicates that $[Mo^{(V)}O_2(OC_6H_4O)_2]^{3-}$ and $[W^{(VI)}O_2(OC_6H_4O)_2]^{2-}$ might have the related coordinated structure feature with the cofactor of flavoenzyme.

Table 1 Crystal data for $(NH_2CH_2CH_2NH_3)_2[W^{(VI)}O_2(OC_6H_4O)_2]$

Formula weight	488.36	Absorption coefficient	57.060 cm^{-1}
Temperature	(299 ± 1) K	$F(000)$	1152
Radiation (Mo Kα)	0.071073 nm	Crystal size	0.20 mm × 0.30 mm × 0.40 mm
Crystal system	monoclinic	$2\theta_{max}$	50°
Space group	$P2_1/c$	Index ranges	$-8 \leqslant h \leqslant 8$, $0 \leqslant k \leqslant 36$,
Unit cell dimensions	$a = 0.7114(1)$ nm		$0 \leqslant l \leqslant 11$
	$b = 3.0768(6)$ nm	Reflection collected	3883
	$c = 0.9755(2)$ nm	Independent reflections	3360
	$\beta = 102.69(3)°$	Data/restraints/parameters	2393/0/262
Volume	2.083(1) nm^3	Goodness-of-fit on F^2	0.98
Z	4	Final R indices $[I > 2\sigma(I)]$	$R_1 = 0.037$, $wR = 0.059$
Density (calculated)	1.857	Largest diff. peak and hole	1.00 and −1940 e·nm^{-3}

Table 2 Selected bond lengths (nm × 10^{-1}) and angles (°) for the title complex

W(1)—O(1)	2.131(5)	W(1)—O(2)	1.983(5)	W(1)—O(3)	2.131(5)
W(1)—O(4)	1.981(5)	W(1)—O(11)	1.744(5)	W(1)—O(12)	1.741(5)
O(1)—C(11)	1.344(8)	O(2)—C(16)	1.367(8)	C(11)—C(12)	1.39(1)
C(11)—C(16)	1.38(1)	C(12)—C(13)	1.45(1)	O(13)—C(14)	1.31(1)
C(14)—C(15)	1.39(1)	C(15)—C(16)	1.37(1)	O(3)—C(21)	1.339(8)
O(4)—C(26)	1.362(8)	C(21)—C(22)	1.38(1)	C(21)—C(26)	1.41(1)
C(22)—C(23)	1.39(1)	C(23)—C(24)	1.39(1)	C(24)—C(25)	1.41(1)
C(25)—C(26)	1.38(1)	N(31)—C(32)	1.43(1)	C(32)—C(33)	1.51(1)
C(33)—N(34)	1.420(9)	N(41)—C(42)	1.446(8)	C(42)—C(43)	1.53(1)
C(43)—N(44)	1.437(9)	C(51)—N(51)	1.422(8)	C(51)—C(51a)	1.52(1)
O(1)-W(1)-O(2)	77.3(2)	O(1)-W(1)-O(3)	80.5(2)	O(2)-W(1)-O(3)	89.3(2)
O(1)-W(1)-O(4)	86.1(2)	O(2)-W(1)-O(4)	159.8(2)	O(3)-W(1)-O(4)	76.2(2)
O(1)-W(1)-O(11)	92.3(2)	O(2)-W(1)-O(11)	102.2(2)	O(3)-W(1)-O(11)	164.9(2)
O(4)-W(1)-O(11)	89.7(2)	O(1)-W(1)-O(12)	162.2(2)	O(2)-W(1)-O(12)	89.2(2)
O(3)-W(1)-O(12)	87.8(2)	O(4)-W(1)-O(12)	104.3(2)	O(11)-W(1)-O(12)	102.0(2)
W(1)-O(1)-C(11)	112.4(5)	W(1)-O(2)-C(16)	117.2(5)	O(1)-C(11)-C(12)	123.5(8)
O(1)-C(11)-C(16)	116.5(8)	C(12)-C(11)-C(16)	120.0(7)	C(11)-C(12)-C(13)	115.2(9)
C(12)-C(13)-C(14)	123.3(8)	C(13)-C(14)-C(15)	121.0(9)	C(14)-C(15)-C(16)	117.6(9)
O(2)-C(16)-C(11)	115.5(6)	O(2)-C(16)-C(15)	121.5(8)	C(11)-C(16)-C(15)	122.9(7)
W(1)-O(3)-C(21)	114.4(4)	W(1)-O(4)-C(26)	118.7(4)	O(3)-C(21)-C(22)	125.5(7)
O(3)-C(21)-C(26)	115.1(6)	C(22)-C(21)-C(26)	119.4(6)	C(21)-C(22)-C(23)	119.6(7)
C(22)-C(23)-C(24)	120.6(7)	C(23)-C(24)-C(25)	120.5(8)	C(24)-C(25)-C(26)	118.5(8)
O(4)-C(26)-C(21)	115.1(6)	O(4)-C(26)-C(25)	123.4(7)	C(21)-C(26)-C(25)	121.5(6)
N(31)-C(32)-C(33)	113.4(6)	C(32)-C(33)-N(34)	116.5(8)	N(41)-C(42)-C(43)	112.5(6)
C(42)-C(43)-N(44)	113.0(6)	N(51)-C(51)-C(51a)	113.7(7)		

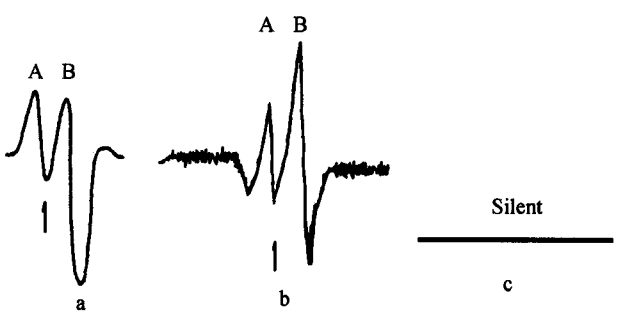

Fig. 3 EPR spectrum of flavoenzyme (a), $[Mo^{(V)}O_2(OC_6H_4O)_2]^{3-}$ (b) and $[W^{(VI)}O_2(OC_6H_4O)_2]^{2-}$ (c).

The different electronic configuration feature between Mo(V) and W(VI) is also reflected in UV-vis spectrum. As shown in Fig. 4, there are one single at 365 nm which associates with catecholate-molybdenum charge transfer and another peak at 280 nm which is assigned to n-π* and π-π* transitions of catecholate ligand in $[Mo^{(V)}O_2(OC_6H_4O)_2]^{3-}$. But there is only a broad peak which covers the range of 280 nm to 365 nm in $[W^{(VI)}O_2(OC_6H_4O)_2]^{2-}$ due to d^0 electronic configuration of W(VI) which might increases the charge transition from catecholato to molybdenum and affects the charge transitions among the catecholate ligand n-π* and π-π* so that

the two peaks at 280 nm and 365 nm are mixed together.

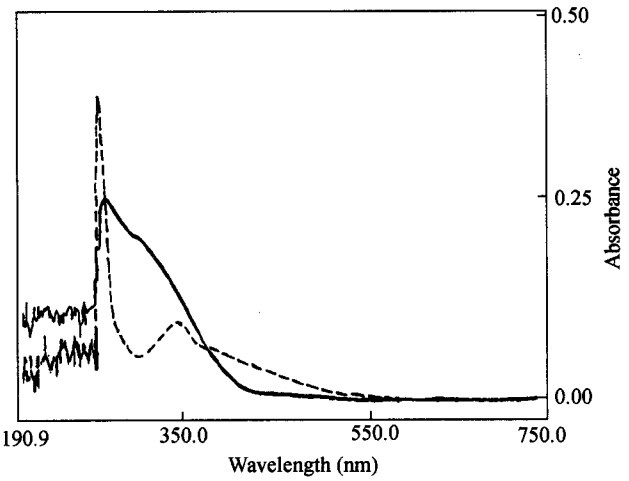

Fig. 4 UV-vis spectrum of $[W^{(VI)}O_2(OC_6H_4O)_2]^{2-}$ (solid line) and $[Mo^{(V)}O_2(OC_6H_4O)_2]^{3-}$ (dashed line) in H_2O.

The ^1H NMR spectra of the pure $(NH_2CH_2CH_2NH_3)_2[W^{(VI)}O_2(OC_6H_4O)_2]$ complex solution prepared freshly are strongly disturbed and all the peaks are broadened greatly, which implicates that there are some paramagnetic substances presented in the system. For $(NH_2CH_2CH_2NH_3)_2[W^{(VI)}O_2(OC_6H_4O)_2]$ crystal, there is no any paramagnetic species because all the electrons are paired already, so it can be deduced that the oxidation state of W(VI) is unstable and the reduction from W(VI) to W(V) occurs in solution. As shown in Fig. 5(a) there is one very strong and broad signal with hyperfine that it is impossible to be assigned according to the AA'BB' spine system of catocholato ligand in the title complex. While it is noteworthy that the paramagnetic effect disappears totally and the resolution and the sensitivity of the peaks are well improved in the ^1H NMR spectra when ATP solution is mixed with the original pure complex solution. It is more worthy to note that the strong and broadened peak decreases in relative intensity as shown in Fig. 5(c), and a new pair of the multiplets appears. The expanded spectra of the multiplets as presented in Fig. 5(d) is almost the same as the ^1H NMR spectra of catechol molecule exhibited in Fig. 6 which illustrates that a part of catecholato ligands decomposed from the central W metal ion in the system. The signal at δ 117.1 decreases greatly in ^{13}C NMR spectra compared with the original spectra confirms that the conclusion deduced from ^1H NMR studies. The result reveals that the central metal ion W(V) is oxidized from W(V) to W(VI) when the pure complex solution is mixed with ATP solution, and all most part of catecholate ligands in the system hydrolizes at mean time.

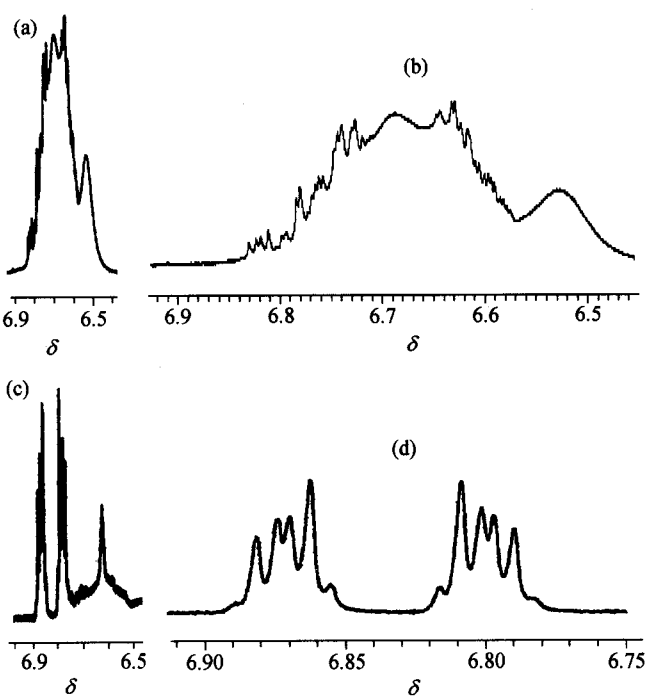

Fig. 5 ^1H NMR spectra of catecholate ligand (a) and the expanded spectra (b) in pure complex solution and the ^1H NMR spectra of catecholate ligand (c) and the expanded spectra (d) in the solution mixed with ATP.

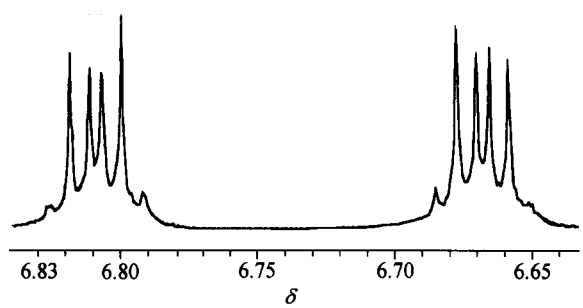

Fig. 6 Expanded ^1H NMR spectra of catechol molecule.

The species $[WO_2]^{2+}$ produced by the dissociation of $[W^{(VI)}O_2(OC_6H_4O)_2]^{2-}$ coordinate with two ethylenediamine N atoms in turn, which can be ruled out from the down-shift of ^1H NMR chemical shift and the up-shift of ^{13}C NMR chemical shift when ATP solution is added. The ^1H NMR chemical shift difference of ethylenediamine H atom between the pure complex solution and the mixed solution is 0.468 given in Table 3 and the ^{13}C NMR chemical shift difference of that is 3.3 listed in Table 5.

From Tables 4 and 6, it can be seen that the ^1H NMR and ^{13}C NMR chemical shifts of ATP mixed with the complex are almost the same as that of pure ATP at same pD in solution, which suggests that W ion in the complex does not coordinated directly to heterocyclic N atoms of ATP. It is in agreement with the coordination structure of cofactor of tungstoenzyme in which the ligand pterin nucleus itself does not ligate directly to the central W metal ion,[6] and W ion does not coordinated directly to phosphate O atoms also. So we can conclude that ATP does not react with the complex by covalent interaction but stabilizes the W(VI) oxidized state of the complex in solution. The mechanism of stability effect of ATP to W(VI) is undertaking.

Table 3 ^{1}H NMR chemical shift of the title complex in the pure complex solution and the solution mixed with ATP

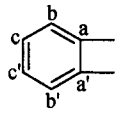

Sample	NCH_2	H-b, H-c	H-b′[a]	H-c′[a]
Lu3	2.897 (s)		6.585—6.811[b](m)	
Lu3 + ATP	3.365 (s)	6.661[c](s)	6.661—6.806 (m)	6.862—6.881 (m)

[a] The hydrolysis product of catecholate ligand; [b] the signals of H-b, H-c, H-b′ and H-c′ are overlapped together; [c] the signals of H_B and H_C are overlapped together.

Table 4 ^{1}H NMR chemical shift of ATP and that in the solution mixed with the complex

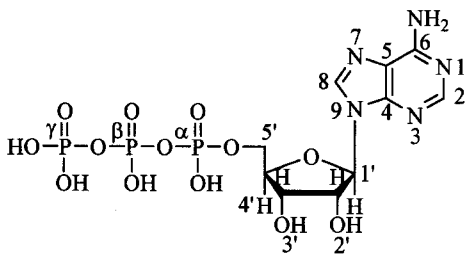

ATP

Sample	H-1′	H-2′	H-3′	H-4′	H-5	H-5′	H-2	H-8
ATP	6.1	4.7	4.5	4.4	4.3	4.3	8.4	8.6
Lu3 + ATP	6.090	4.736	4.541	4.378	4.235	4.235	8.194	8.474

Table 5 ^{13}C NMR chemical shift of the title complex and that in the solution mixed with ATP

Complex	NCH_2	C-c, C-b	C-c′	C-b′	C-a
Lu3	43.2	117.7	119.2	123.0	157.9?
Lu3 + ATP	39.9	117.1	119.4	124.2	157.9

Table 6 ^{13}C NMR chemical shift of ATP and that in the solution mixed with the title complex

ATP	C-5′	C-3	C-2	C-4	C-1′	C-5	C-8	C-2	C-4	C-6
ATP	68.2	73.3	78.9	87.2	90.8	121.3	145.2	148.6	151.2	153.2
Lu3 + ATP	68.4	73.4	77.5	87.1	90.0	121.6	143.2	147.0	152.0	155.0

References

1 Hille, R. *Chem. Rev.* **1996**, *96*, 2757.
2 Mader, M. L.; Carducci, M. D.; Enemark, J. H. *Inorg. Chem.* **2000**, *39*, 525.
3 Holm, R. H. *J. Am. Chem. Soc.* **1998**, *120*, 3259.
4 Lim, B. S.; Donahue, J. P.; Holm, R. H. *Inorg. Chem.* **2000**, *39*, 263.
5 Schindelin, H.; Kisker, C.; Hilton, J.; Rajagopalan, K. V.; Rees, D. C. *Science* **1996**, *272*, 1615.
6 Johnson, M. K.; Ress, D. C.; Adams, M. W. W. *Chem. Rev.* **1996**, *96*, 2817.
7 Sung, K. M.; Holm, R. H. *Inorg. Chem.* **2000**, *39*, 1275.
8 Wong, Y.-L.; Yan, Y.-E.; Chan, S.-H.; Yang, Q.-C.; Mak, T. C. W.; Ng, D. K. P. *J. Chem. Soc., Dalton Trans.* **1998**, *18*, 3057.
9 Donahue, J. P.; Lorber, C.; Nordlander, E.; Holm, R. H. *J. Am. Chem. Soc.* **1998**, *120*, 102.
10 Lu, X.-M.; Liu, S.-C.; Mao, X.-A.; Bu, X.-H. *J. Mol. Struct.* **2001**, *562*, 89.

(E0210156 CHENG, B.)